

# An innovative experimental device for characterizing the responses of monopiles subjected to complex lateral loading

Zitao Zhang<sup>1#</sup>, Wei Wang<sup>2</sup>, Xuedong Zhang<sup>1</sup>, Guangming Yu<sup>2</sup>, and Jing Hu<sup>1</sup>

<sup>1</sup> State Key Laboratory of Simulation and Regulation of Water Cycle in River Basin, China Institute of Water Resources and Hydropower Research, Beijing, China.

<sup>2</sup> China Three Gorges Corporation, Beijing, China

<sup>#</sup>Corresponding author: [zhangzt@iwahr.com](mailto:zhangzt@iwahr.com)

## ABSTRACT

Offshore wind turbines are usually founded on monopiles. During the operation period, the structure is subjected to complex lateral loading from wind, wave and current. The soils surrounding those monopiles may deform with increasing the number of loading cycles, leading to tilting of the whole structure; hence, it is vital to carry out physical model tests to examine the long-term performance of monopiles. This study proposes an innovative experimental setup for centrifuge modelling of the response of monopiles under complex lateral loading. Hydraulic actuators are adopted to apply lateral loads on model pile, and electrohydraulic servo-valves and associated controllers are used to achieve a closed loop position or load control. A carefully designed spherical hinge and load bars are used to connect the model pile and actuator shafts. This enables that the pile can rotate freely and can move vertically freely. A centrifuge test on a winged monopile subjected to perpendicular lateral loading was carried out at 100g. The experimental results shed light on pile responses in the cyclic loading and constant loading directions.

**Keywords:** centrifuge testing; piles; complex loading.

## 1. Introduction

Monopiles which are widely used to support offshore wind turbines are subjected to complex lateral loading from wind, wave and current (Martínez-Chaluisant et al. 2010). The direction, magnitude and frequency of the lateral loading keep changing over time (Richards et al. 2020). The soils surrounding those monopiles may deform with increasing the number of loading cycles, leading to tilting of the whole structure. According to Chinese code for design of wind turbine foundations (NEA 2019), the rotational angle of monopiles in the seabed level should not exceed 0.5° during the whole operation period. Therefore, it is important to examine the behaviour of monopiles subjected to complex lateral loading.

This study proposes an innovative experimental setup for centrifuge modelling of monopiles. The setup is used to explore the ratcheting behaviour of winged monopiles under perpendicular lateral loading.

## 2. Brief review of devices for physical modelling of monopiles

Table 1 summarizes the devices for physical modelling of monopiles. LeBlanc et al. (2010) used a mass connected with pile head using a wire and pulley system. Unidirectional cyclic loading can be applied on pile head by rotating the mass with a motor. Only sinusoidal load can be achieved as the constant rotational

velocity of the mass. In Richards et al. (2020), the monopiles are subjected to more complex multi-directional loading using two perpendicular electric actuators.

The afore-mentioned tests were carried out at 1g conditions, where g is gravitational acceleration. Similar tests were also performed in centrifuge. In Rudolph et al. (2014), the pile head is connected with an output shaft of a vertically installed actuator through a wire and pulley system. The system translates the vertical movement of the actuator into horizontal loading at pile head. Meanwhile, the change of loading direction is realized by moving the actuator horizontally. Bayton et al. (2018) used two pneumatic actuators to apply unidirectional cyclic loading and monotonic loading simultaneously on the pile at different elevations. Truong et al. (2018) performed both drum and beam centrifuge tests. In drum centrifuge tests, a loading arm with a wheel end was used to apply lateral load on pile head, which allowed free rotation of the head. However, only one-way loading can be achieved in this device. In beam centrifuge tests, a horizontal load motor and an installation motor were used to achieve inflight pile installation and subsequent lateral loading without ramping down the centrifuge. A hinge was mounted at pile head to allow rotation of model piles under lateral load. However, pile head was fixed in the vertical direction, which was different from the prototype conditions.

**Table 1.** Summary of devices for physical modelling of monopiles

Reference	Load type	Actuator Number and type	$N$	$D_p$ (mm)
LeBlanc et al. (2010)	Unidirectional sinusoidal load	1 electric	1	80
Richards et al. (2020)	Unidirectional, multi-directional and multi-amplitude storm load	2 electric	1	80
Rudolph et al. (2014)	Varying loading direction	Not presented	200	25
Bayton et al. (2018)	Unidirectional loads at 2 different elevations	2 pneumatic	100	50
Truong et al. (2018)	Unidirectional load (only one-way), Drum centrifuge	1 (the type is not presented)	250	11
	Unidirectional load, Beam centrifuge	2 electric (one for pile installation)	60	40
<b>This study</b>	Multi-directional load	2 hydraulic	100	90

### 3. Development of the device for centrifuge modelling of monopiles

#### 3.1. Overall arrangement

An innovative device for centrifuge modelling of monopiles was designed and manufactured by China Institute of Water Resources and Hydropower Research (IWHR) and Beijing Jijian Technology Co., Ltd. The device is installed on the 400g-t beam centrifuge at IWHR. The advanced centrifuge has both normal-speed and high-speed operation modes. In normal-speed mode, the maximum centrifugal acceleration is 200g and the maximum payload is 2 t. In high-speed mode, the maximum centrifugal acceleration is as high as 1000g while the maximum payload is only 0.4 t. The device for physical modelling of monopiles is used when the centrifuge operates in the normal-speed mode.

The device comprises six parts, i.e., (1) soil container and model pile; (2) loading frame and hydraulic actuators; (3) connections between model pile and actuators; (4) servo-valves, controllers and lower computer; (5) upper computer; and (6) hydraulic station. As shown in Fig. 1, the parts (1), (2) and (3) are in the test basket of the centrifuge, while part (4) is installed in the cabinet near rotational axis. All those components are distributed in the centrifuge cabin at floor B1. Part (5) is in the control room at floor 1, and the communication between upper and lower computers are achieved using fiber optic rotary joints. The hydraulic station at floor B2 is connected with the supply and return oil lines in the centrifuge through pipes and fluids rotary joints.

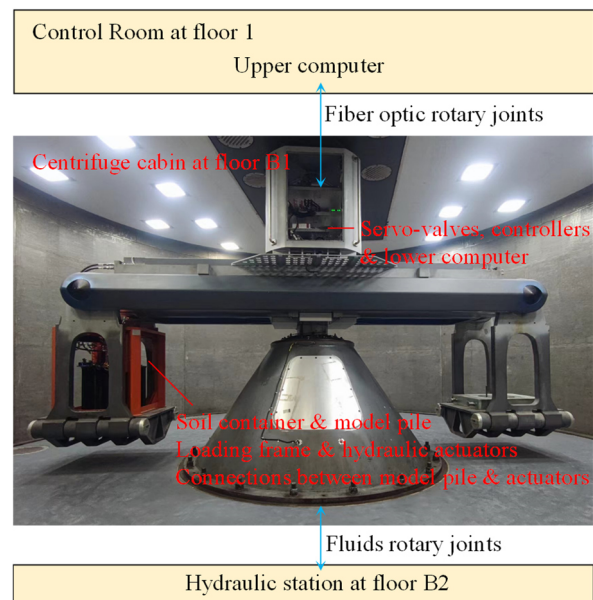


**Figure 1.** Overall arrangement of the device.

#### 3.2. Soil container and model pile

The soil container has an internal diameter of 700 mm and internal height of 680 mm. The model pile is made of circular aluminum tube, which has an inner diameter of 84 mm and an outer diameter ( $D_p$ ) of 90 mm. For a test carried out at 100g, the prototype pile diameter reaches 9 m, which is much larger than that used in previous centrifuge tests (see Table 1). Moreover, four aluminum plates are installed on the tube to model the winged monopile. In order to monitor pile rotation, four laser displacement sensors were installed around the pile (see Fig. 2). As the surface curvature of the model pile may bias the measurement of horizontal displacement, two thin aluminium plates are mounted on the model pile.

#### 3.3. Loading frame and hydraulic actuators

As shown in Figs. 2 and 3, the loading frame comprises a base part and a moving crosshead. The base part is mainly composed of a bottom plate and four columns, and ribbed plates and beams are installed near the top and bottom of the columns to increase its stiffness. The base part has a width of 1218 mm and a height of 1294 mm. Two perpendicularly oriented hydraulic actuators are mounted on the crosshead. The height from base place surface to each axis of the actuator shaft is adjustable. The minimum and maximum heights are 634 mm and 1134 mm, respectively. Both hydraulic actuators are identical, and each one has a stroke of 120 mm and a maximum load of 10 kN. For a test carried out at 100g, the prototype horizontal displacement of pile head reaches 12 m, and the maximum prototype load applied on pile head is 100 MN.

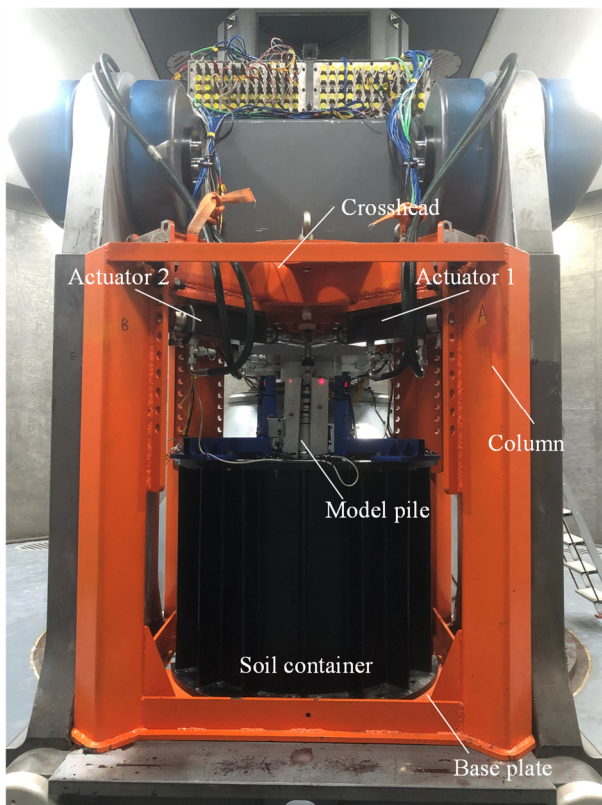


**Figure 2.** Soil container, loading frame and actuators.

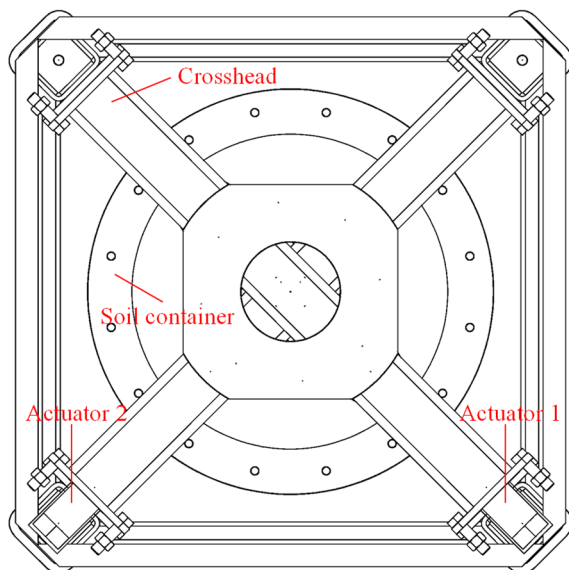


**Figure 3.** Plan view of the loading frame.

### 3.4. Connections between actuator and the model pile

As shown in Fig. 4, a spherical hinge is mounted on pile head. The lower shaft end of the hinge is inserted to the model pile, which enables transfer of horizontal force and moment between the shaft end and model pile. The upper shaft end of the spherical hinge is connected with the actuator shafts. As a hinge is used in the connection between each actuator shaft and the associated load bar, each load bar can rotate freely along a vertical axis in the hinge. The other end of each load bar contains a hole, and the upper shaft end of the spherical hinge is inserted into

the holes of load bars. The load bars can rotate freely along the axis of the upper shaft end. Meanwhile, the upper shaft end can move freely in the vertical direction; hence, the vertical movement of the model pile is not restricted, which is similar to the prototype conditions.

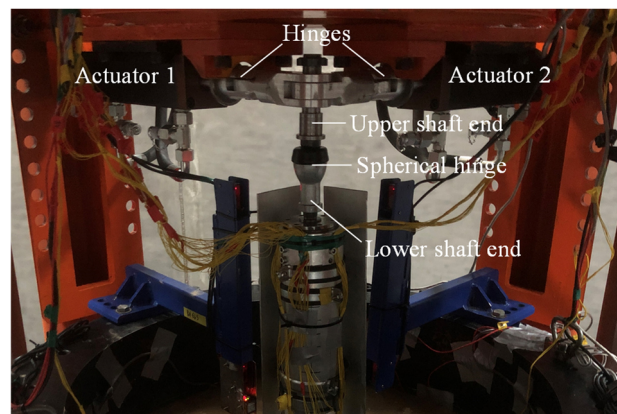


**Figure 4.** Connections between actuator and the model pile.

### 3.5. Servo-valves and controllers

Mechanical Feedback (MFB) electrohydraulic servo-valves (model 761, Moog Inc.) are used to adjust flow to the hydraulic actuators. Each servo-valve's two output control ports are connected across a hydraulic actuator. Meanwhile, each servo-valve is connected with a controller to achieve a closed loop position or load control. Taking position control as an example, position command is generated by the control motion cards in the controller. The controller then sends a command signal to the servo-valve and drive the actuator to a new position, which is monitored by a position transducer installed in the actuator. The output of this transducer is compared with the command input in the controller, the deviation is amplified and fed to the servo-valve as a command signal. The flow to the actuator is adjusted until the position output agrees with the command input. The closed loop force control is similar to the position control, the only difference is that a full bridge of strain gauges mounted on the surface of model pile is used to monitor the present lateral load.

### 3.6. Hydraulic station

The hydraulic station has an oil pressure up to 10 MPa and a flow rate up to 70 L/min. In addition, the hydraulic station is equipped with an oil filter and bladder accumulator.

### 3.7. Vacuum saturation apparatus

In order to saturate the soil sample, a vacuum saturation apparatus is developed. As shown in Fig. 5, the soil container is assembled with a cover with an O-ring, creating sealed space in the container. A relative vacuum is generated in the space by a vacuum pump, and a peristaltic pump is used to move fluids from the liquid container to the base of the soil sample. The flow rate is usually controlled as low as 0.3 kg/h to prevent fluidization of the soils.



**Figure 5.** Vacuum saturation device.

### 3.8. Pile installation frame

As shown in Fig. 6, a top beam is mounted on the base part of the loading frame to form a support structure for model pile installation. A lead screw rod with a hand wheel is installed in the center of the top beam to facilitate the adjustment of the rod locations. A hydraulic cylinder equipped with a manual hand pump is used to install the model pile. The cylinder has a capacity of 10 t and a stroke of 50 mm. A pile guiding and positioning frame is used to ensure accurate positioning of the model pile.



**Figure 6.** Pile installation frame.

## 4. Experimental details

A centrifuge tests on a model winged monopile was carried out in this study. The centrifugal acceleration used in the test was 100g.

### 4.1. Sample preparation

The sandy soil used in this study is a mixture of silica sands collected from Fujian Province, China and aeolian soils collected from Xinjiang Province, China. It contains 57% of silica sands ranging in size from 0.106 to 0.212 mm and 43% of aeolian soils. Those aeolian soil particles are smaller than 2 mm, while 97.9% are smaller than 0.075 mm, and 8% are smaller than 0.005 mm. The minimum and maximum void ratios of the sandy soils are 0.44 and 1.22, respectively. The minimum and maximum dry densities are 1.19 and 1.84 g/cm<sup>3</sup>, respectively.

As shown in Figs. 7 and 8, a 10-mm thick layer of dry gravels ranging in size from 2 to 4 mm were firstly prepared in the soil container to facilitate soil saturation. The dry sandy soils were then placed layer by layer above the gravels, and the dry density was controlled as 1.49 g/cm<sup>3</sup>. The initial total thickness of the sandy soils was 510 mm. The dry sample were then saturated using the vacuum saturation apparatus. Afterwards, the soil sample was transferred to the centrifuge basket and was consolidated at 100g. After consolidation, the height of the sandy soils became 490 mm, corresponding to 49 m at prototype scale. The achieved dry density was 1.55 g/cm<sup>3</sup>, corresponding to a relative density of 62%.

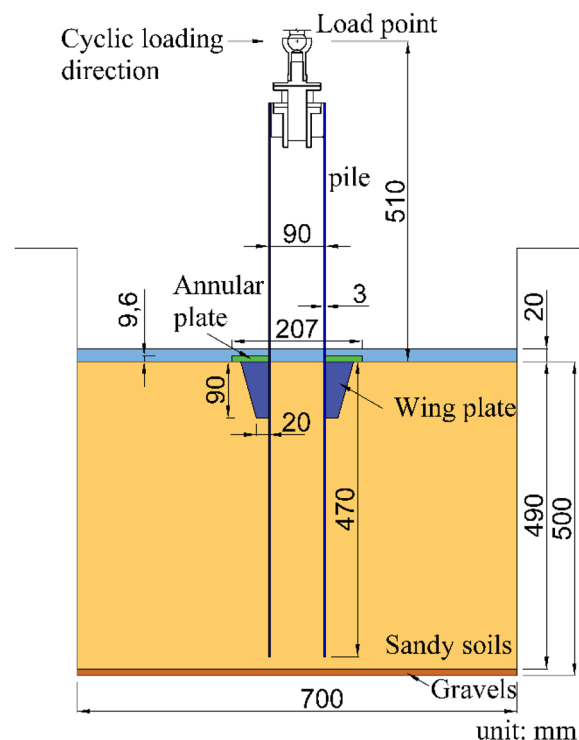


**Figure 7.** Section view of the centrifuge model

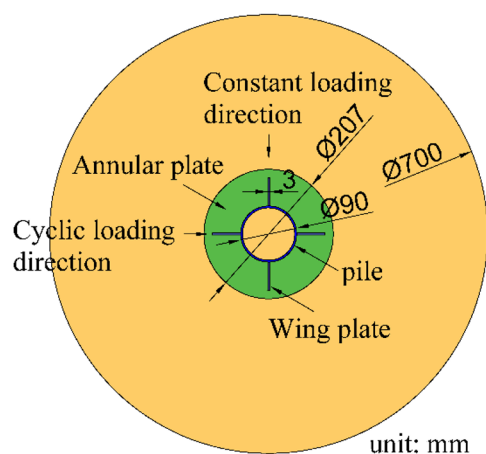


**Figure 8.** Plan view of the centrifuge model

#### 4.2. Model pile installation

After soil consolidation, the model winged monopile with a diameter  $D_p$  of 90 mm described in clause 3.2 was penetrated into the sandy soils using pile installation frame at 1g. The embedment depth  $L$  was 470 mm, corresponding to 47 m at prototype scale. The ratio of  $L/D_p$  was 5.2. The load point is located at the center of the spherical hinge. The height from the soil surface to the load point, i.e., the eccentricity,  $e$ , is 510 mm. This corresponded to 51 m at prototype scale, and the ratio of  $e/D_p$  was 5.7. After pile installation, an annular aluminum plate was put above the soil sample around the pile. The plate had an outer diameter of 207 mm and a thickness of 9.6 mm. This was used to reproduce the vertical loading applied on the soil surface by cemented gravels used in scour counter measures.

#### 4.3. Testing procedures

Perpendicular cyclic loading tests were performed at 100g. As commented by Richards et al. (2020), perpendicular loading tests may provide fundamental insight and may also represent misaligned wind and wave loading in the field. As shown in Fig. 9, cyclic loading was applied in  $x$ -direction, while the loading in  $y$ -direction remained constant. As illustrated in Table 2, five groups of loading cycles were tested, and each group contained 2000 cycles. There were in total 10,000 loading cycles. The same mean horizontal forces were applied in both directions in each group, which was defined as L-shape tests in Richards et al. (2020). The cyclic loading frequency increased from 1 to 4 Hz in the initial 400 cycles in Group 1, and then 4 Hz was used in the following 1600 cycles in Group 1 and in other groups. The mean force decreased from 0.32 kN to 0.16 kN from groups 1 to 3, and then the value increased to 0.32 kN in group 5. The cyclic force amplitudes increased from 0.24 kN to 0.72 kN from groups 1 to 3, and then the value decreased to 0.24 kN in group 5.

**Table 2.** Sequence of loading cycles

Group No.	Mean force in x-direction (kN)	Amplitude in x-direction (kN)	Force in y-direction (kN)
1	0.32	0.24	0.32
2	0.24	0.48	0.24
3	0.16	0.72	0.16
4	0.24	0.48	0.24
5	0.32	0.24	0.32

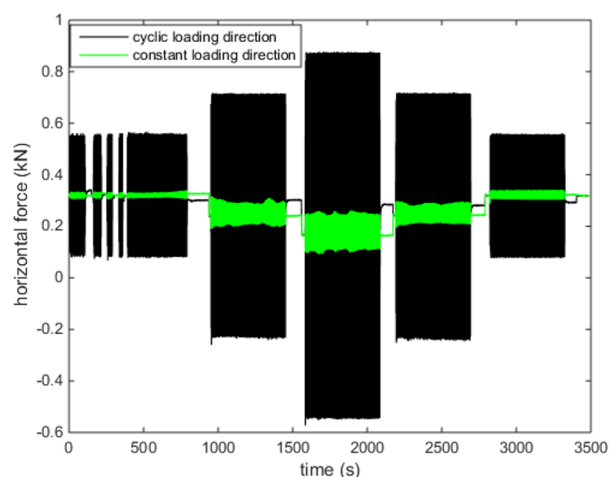


**Figure 9.** Time series of measured horizontal forces.

### 5. Experimental results

#### 5.1. Response in the cyclic loading direction

Fig. 10 presents the measured displacements in cyclic loading direction at different elevations. Pile head moves towards the direction of average loads with increasing cycle number. The displacements are first used to calculate rotational angles, which are illustrated in Fig. 11. The rotational angle increases with increasing cycle number. The rotational angle increments due the cyclic loading in groups 1, 2 and 3 are  $0.020^\circ$ ,  $0.027^\circ$  and  $0.034^\circ$ , respectively. However, the increments in groups 4 to 5 are as small as  $0.005^\circ$ . This suggests the effect of previous cyclic loading on the ratcheting response. The same behavior can be clearly shown in the relationship between horizontal force and rotational angle. As shown in Fig. 12, although the average loads are the same in groups 1 and 5, the development in rotational angle is relatively small in group 5. Similarly, the rotational angle in group 4 is much smaller than that observed in group 2.

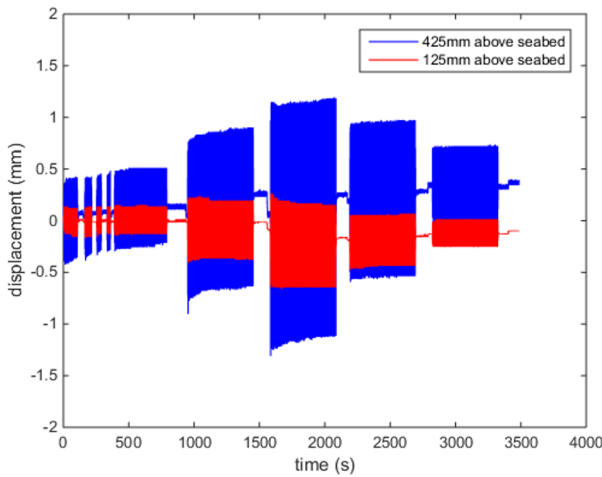


**Figure 10.** Pile displacements in cyclic loading direction.

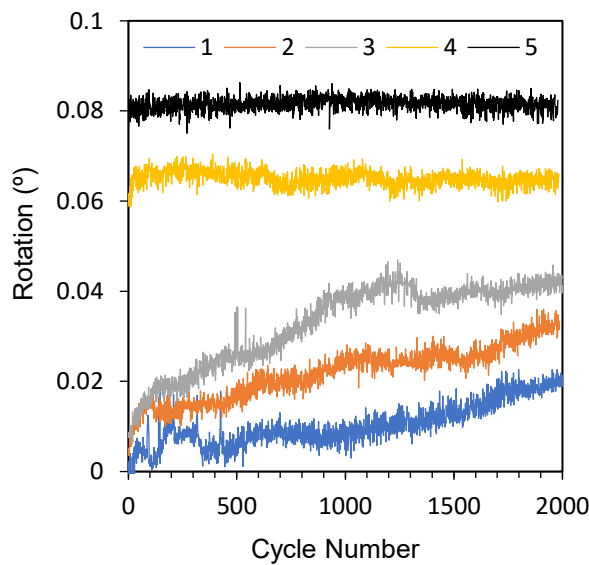


**Figure 11.** Rotations in cyclic loading direction.

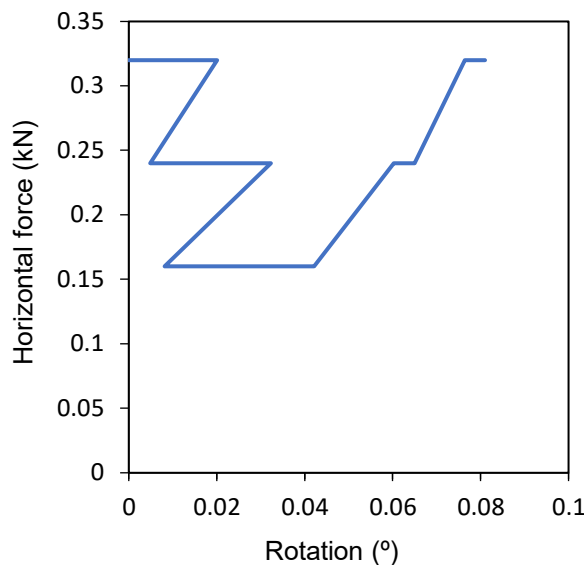


**Figure 12.** Relationship between horizontal force and rotational angle in the cyclic loading direction.

## 5.2. Response in the constant loading direction

As shown in Fig. 13, pile head moves towards the constant loading direction. The rotational angle increments due to the cyclic loading in groups 1 to 3 are  $0.005^\circ$ ,  $0.016^\circ$  and  $0.016^\circ$  respectively (see Figs. 14 and 15). However, the increments in groups 4 to 5 are reduced to  $0.004^\circ$  and  $0.003^\circ$ , respectively. This also suggests the effect of previous cyclic loading on the ratcheting response. In addition, the ratios of the rotational angle increment in constant loading direction over the increment in cyclic loading direction are 28%, 57%, 47%, 86% and 69% in groups 1 to 5, respectively. This suggests that pile head rotates towards a direction between the direction of mean loads and the cyclic loading direction.

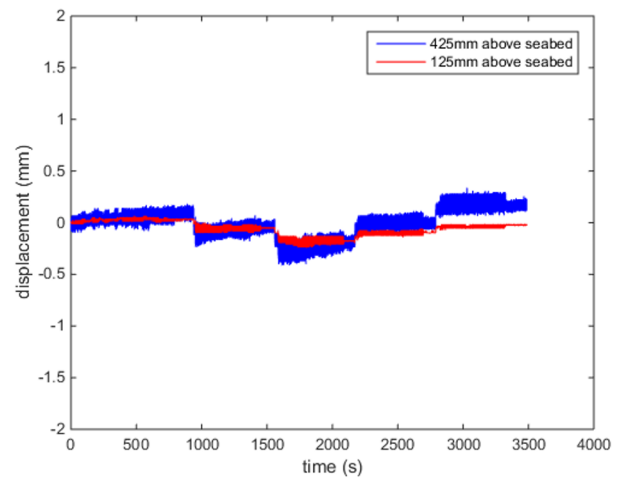


**Figure 13.** Pile displacements in constant loading direction.

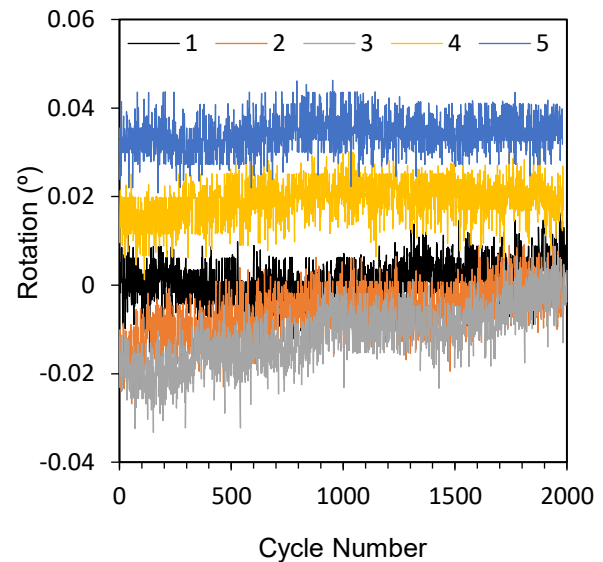


**Figure 14.** Rotations in constant loading direction.

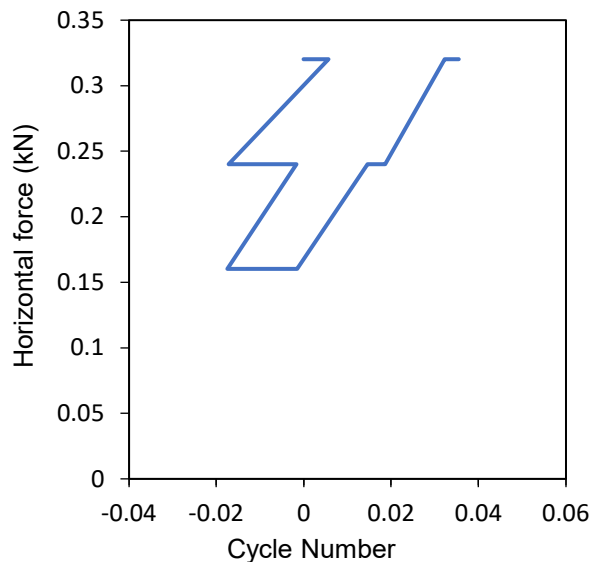


**Figure 15.** Relationship between horizontal force and rotational angle in the constant loading direction.

## 6. Conclusions

An innovative experimental device was developed in this study to characterize the responses of monopiles subjected to complex lateral loading. Hydraulic actuators are adopted to apply lateral loads on model pile, and MFB electrohydraulic servo-valves and controllers are used to achieve a closed loop position or load control. A carefully designed spherical hinge and load bars are used to connect the model pile and actuator shafts. This enables that the pile can rotate freely and can move vertically freely. A centrifuge test on a winged monopile was carried out at 100g. The experimental results indicate that pile head rotates towards a direction between the direction of mean loads and the cyclic loading direction. The results also suggest significant effect of previous cyclic loading on the ratcheting response. This study proves the ability of the proposed device, and more centrifuge tests will be carried out in the future to she

light on the behaviour of monopiles under complex lateral loading.

## Acknowledgements

This research was supported by Research Fund Program of China Three Gorges Corporation (202103016) and National Natural Science Foundation of China (51809290).

## References

- Bakmar, C. L., G. T. Houlsby, and B. W. Byrne. 2010. "Response of Stiff Piles in Sand to Long-Term Cyclic Lateral Loading." *Géotechnique*, 60, no. 2, 79–90.
- Bayton, S. M., J. A. Black, and R. T. Klinkvort. 2018. "Centrifuge Modelling of Long Term Cyclic Lateral Loading on Monopiles. In Proceedings of the 9th International Conference on Physical Modelling in Geotechnics, London, UK, 689–694. CRC Press.
- Martínez-Chaluisant, V., J. A. Schneider, and D. Fratta. 2010. "Physical modeling of the dynamic response of offshore wind turbines founded on monopiles." *Earth and Space 2010: Engineering, Science, Construction, and Operations in Challenging Environments*. 2079–2086.
- National Energy Administration (NEA). 2019. "Code for design of wind turbine foundations of offshore wind power projects (NB/T 10105—2018)." China Water & Power Press, Beijing, China.
- Richards, I. A., B. W. Byrne, and G. T. Houlsby. 2018. "Physical Modelling of Monopile Foundations Under Variable Cyclic Lateral Loading." In *Physical Modelling in Geotechnics*, 737–741. CRC Press.
- Richards, I. A., B. W. Byrne, and G. T. Houlsby. 2020. "Monopile Rotation Under Complex Cyclic Lateral Loading in Sand." *Géotechnique*, 70, no. 10, 916–930.
- Rudolph, C., J. Grabe, and B. Bienen. 2014. "Response of Monopiles Under Cyclic Lateral Loading with A Varying Loading Direction." In *Proceedings of the 8th International Conference on Physical Modelling in Geotechnics, Perth, Australia*, 453–458. CRC Press.
- Truong, P., B. M. Lehane, V. Zania, and R. T. Klinkvort. 2019. "Empirical approach based on centrifuge testing for cyclic deformations of laterally loaded piles in sand." *Géotechnique*, 69, no. 2, 133–145.